ASIAN JOURNAL OF CHEMISTRY

Electrochemical Behaviours and Electrocatalytic Properties of the PW$_{12}$O$_{40}^{3-}$ (Collagen-PW$_{12}$O$_{40}^{3-}$)$_n$/Cysteamine Modified Gold Electrode

L. Liu, Y.H. Song, C.Y. Chen, M. Zhang, H.Z. Yuan and L. Wang*

College of Chemistry and Chemical Engineering, Jiangxi Normal University, Nanchang 330022, P.R. China

*Corresponding author: Tel/Fax: +86 791 8120861. E-mail: lwang@jxnu.edu.cn

A novel multilayer of the type I collagen and PW$_{12}$O$_{40}^{3-}$ was successfully constructed on cysteamine modified gold electrode. Electrochemistry and atomic force microscopy (AFM) were used to characterize the PW$_{12}$O$_{40}^{3-}$ (collagen-PW$_{12}$O$_{40}^{3-}$)n multilayer modified gold electrode. Atomic force microscopy images showed that the PW$_{12}$O$_{40}^{3-}$ preferentially deposited on the collagen network to produce the three-dimensional PW$_{12}$O$_{40}^{3-}$ network. Electrochemical results indicated that the modified electrode exhibited good electrochemical behaviours and electrocatalytic activity towards the reduction of NO$_2^-$. The electrochemical behaviours and electrocatalytic properties of the modified electrode were investigated in detail.

Key Words: Electrochemistry, Electrocatalysis, Collagen, PW$_{12}$O$_{40}^{3-}$, NO$_2^-$.

INTRODUCTION

Polyoxometalates (POMs) have attracted much attention not only due to their especially intrinsic structure[1,2] but also due to their potential application in the field of material science, catalysis, biology and medicine[3-7]. Polyoxometalates, as a class of structurally well-defined anionic clusters with an enormous disparity in size, composition and function, can accept and release several electrons, which makes these compounds very suitable candidates in electrode modification and electrocatalytic research[8-10].

Some methods have been exploited to attach polyoxometalates to the surface of various electrodes, such as adsorption[11], electrochemical deposition[12], incorporation into conductive polymeric matrices[13] and layer-by-layer (LBL) deposition[14-16]. Among these methods, electrochemical deposition has been become a popular method owing to its properties of quick assembly and simple operation. By this method, polyoxometalates have been successfully attached to cysteine[17], cysteamine[18] and poly(ferrocenylsilane)[19] modified electrode.

Type I collagen is composed of right-handed supercoils of three left-handed polyproline helices with major sequences of (Gly-Pro-Hyp)$_n$[20,21]. Under acidic circumstance (pH ≤ 3.5) and low ionic strength, type I collagen molecules could form stationary solution under any temperature[22]. The collagen molecule could also self-assemble into various structures on a solid surface. Whereas these structures strongly depended on temperature. For example, the fibrils and some films with various

densities could form at various temperatures. Generally, the density of collagen film increased as the temperature increased. When the temperature is below the physiological level and the concentration of collagen is below 0.3 mg/mL, it will form a network film with the low packing density. Therefore, type I collagen has been extensively employed to modify surface. For example, type I collagen has been used to construct collagen-silver nanoparticles multilayer for the application in surface-enhanced Raman spectrum[23]. The type I collagen network on an electrode surface was used to control the formation of silver nanoparticles during the electrodeposition process[24]. Even if, some collagen mimics with redox centers (ferrocene) have been synthesized to modify an electrode[25].

In this work, the type I collagen network was used to modify electrode and then PW$_{12}$O$_{40}^{3-}$ was electrodeposited on the collagen network. By recycling the assembly of collagen and electrodeposition of PW$_{12}$O$_{40}^{3-}$, the Au electrode modified with PW$_{12}$O$_{40}^{3-}$(collagen-PW$_{12}$O$_{40}^{3-}$)$_n$ was successfully fabricated. There are two advantages in the fabrication of the PW$_{12}$O$_{40}^{3-}$(collagen-PW$_{12}$O$_{40}^{3-}$)$_n$ modified electrode. For one thing, the type I collagen molecules will be protonated to become anion in acidic conditions and so the negatively charged PW$_{12}$O$_{40}^{3-}$ can strongly adsorb on it. The strong electrostatic interaction between positively charged collagen and negatively charged PW$_{12}$O$_{40}^{3-}$ will enhance the stability of the modified electrode. The other thing, the type I collagen can form three-dimensional network film. So it can not only elevate PW$_{12}$O$_{40}^{3-}$ on the electrode surface but also improve

the electrolyte ion transfer so as to enhance electron transfer in the multilayer. The resulted electrode exhibited good electrochemical behaviours and electrocatalytic properties towards the reduction of nitrite. The electrochemical and electrocatalytic properties of the modified electrode were investigated in detail.

EXPERIMENTAL

Type I collagen from calf skin and cysteamine were purchased from Aldrich-Sigma. $PW_{12}O_{40}^{3-}$ was obtained from Beijing Pure Chemical Plant (China). Other chemicals were purchased from Beijing Chemical Reagent Factory (Beijing, China) and were of analytical grade. All the reagents were used as received without further purification. The aqueous solutions were prepared with triple-distilled water.

All electrochemical experiments were performed by a CHI 430A electrochemical workstation (Shanghai, China). A conventional three-electrode system was used with $PW_{12}O_{40}^{3-}$ (collagen-$PW_{12}O_{40}^{3-}$)$_n$/cysteamine/Au electrode as working electrode, a platinum wire as auxiliary electrode and a saturated calomel electrode (SCE) as reference electrode. The auxiliary electrode, SCE and the naked Au electrode were purchased from CHI (Shanghai, China). Magnetic stirrer (IKA RH bascic 1) was used to stir the solution. All experiments were carried out in 0.1M H_2SO_4 solution at room temperature. Electrolyte solutions were purged with high purity nitrogen prior to experiments and blanketed with nitrogen during electrochemical experiments.

Atomic force microscopy (AFM) measurements were carried out with an AJ-III (Shanghai Aijian Nanotechnology) in tapping mode. Standard silicon cantilevers (spring constant, 0.6-6.0 N/m) were used under its resonance frequency (typically, 60-150 kHz) at room temperature under ambient condition.

Fabrication of $PW_{12}O_{40}^{3-}$ (collagen-$PW_{12}O_{40}^{3-}$)$_n$/cysteamine/Au electrode: Gold electrode was polished with 1, 0.3 and 0.05 μm Al_2O_3 powders to obtain a mirror-like surface before experiments and then was rinsed with triple-distilled water and absolute ethanol in an ultrasonic bath for 3 min, respectively. The polished electrode was immersed in a 1 mM ethanol solution of cysteamine for 24 h and followed by ultrasonicating with absolute ethanol and by rinsing with triple-distilled water to remove off the unbound cysteamine from the surface of gold electrode. Subsequently, the cysteamine modified gold electrode was placed into a 0.1M H_2SO_4 solution containing 1.0 mM $PW_{12}O_{40}^{3-}$ and was cycled for 50 times in the potential range of -0.2-0.8 V at 100 mV/s. Then the type I collagen (0.1 % solution in 0.1 M acetic acid) was dropped on the prepared electrode and dried for 4 h, which formed the collagen/ $PW_{12}O_{40}^{3-}$/cysteamine/Au electrode. Finally, the assembly of collagen and electroadsorption of $PW_{12}O_{40}^{3-}$ were repeated and produced $PW_{12}O_{40}^{3-}$ (collagen-$PW_{12}O_{40}^{3-}$)$_n$/cysteamine/Au electrode. The constructed process was illustrated in Fig. 1.

RESULTS AND DISCUSSION

Atomic force microscopic images: Fig. 2 shows the surface morphologies of the bare Au substrate and $PW_{12}O_{40}^{3-}$ (collagen-
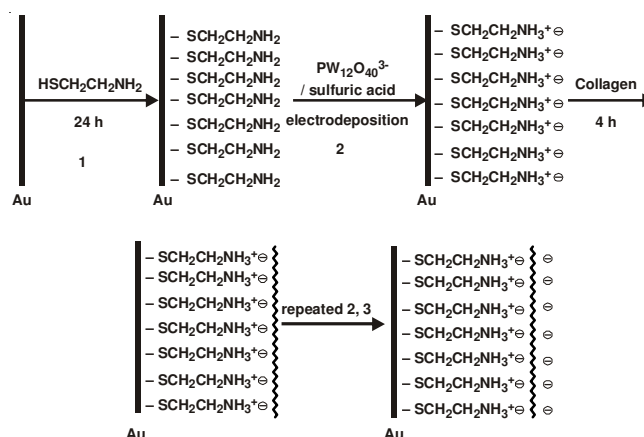

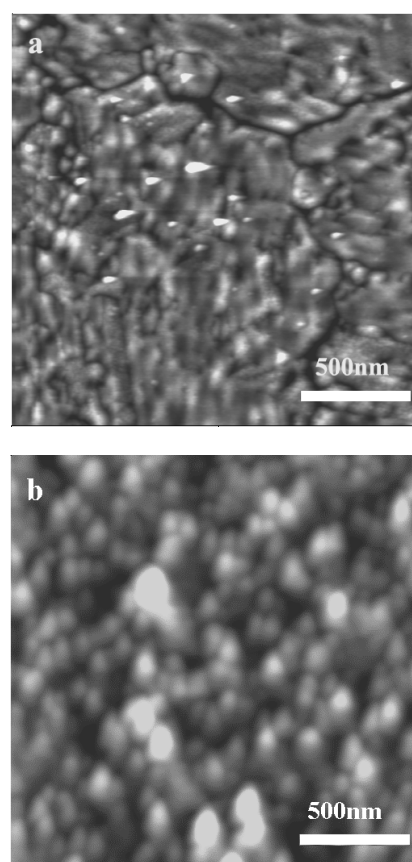Fig. 1. Schematic representation of the procedure for the electrode construction

Fig. 2. AFM images of bare Au substrate (a) and $PW_{12}O_{40}^{3-}$ (collagen-$PW_{12}O_{40}^{3-}$)$_4$/cysteamine/Au electrode (b). The z range: 10 nm (a) and 20 nm (b)

$PW_{12}O_{40}^{3-}$)$_4$/cysteamine/Au electrode. The AFM image of the bare gold substrate presented a smooth and homogeneous surface. Its root-mean-square (RMS) value of the surface roughness was 1.23 (Fig. 2a). After the type I collagen and $PW_{12}O_{40}^{3-}$ were deposited onto the gold substrate, the $PW_{12}O_{40}^{3-}$ (collagen-$PW_{12}O_{40}^{3-}$)$_4$/cysteamine/Au electrode exhibited three-dimensional (3D) porous structure with some small particles (Fig. 2b). The small particles could be ascribed to the cluster of $PW_{12}O_{40}^{3-}$. The RMS value of the surface roughness was inreased to 2.74 nm for $PW_{12}O_{40}^{3-}$ (collagen- $PW_{12}O_{40}^{3-}$)$_4$/cysteamine/Au substrate. These results suggested that the collagen and $PW_{12}O_{40}^{3-}$ were successfully assembled on the

gold substrate and formed three-dimensional porous films. The fabrication of the modified electrode is mainly based on the electrostatic interaction between PW$_{12}$O$_{40}^{3-}$ and the collagen. Under acidic condition, -NH$_2$ of the collagen molecules would accept a proton and became NH$_3^+$. The positive NH$_3^+$ was helpful to attract negative PW$_{12}$O$_{40}^{3-}$ anion. When the PW$_{12}$O$_{40}^{3-}$/cysteamine/gold electrode was dipped into acetic acid solution of collagen, the positive collagen molecules could strongly adsorb on the PW$_{12}$O$_{40}^{3-}$/cysteamine/gold electrode and form network film. Subsequently, the PW$_{12}$O$_{40}^{3-}$ preferentially electrodeposited on the collagen networks to produce PW$_{12}$O$_{40}^{3-}$ networks in the electrochemically cyclic sweeps. As a result, the fabrication of PW$_{12}$O$_{40}^{3-}$ (collagen-PW$_{12}$O$_{40}^{3-}$)$_4$/cysteamine/Au substrate could be constructed successfully.

Electrochemical behaviours of PW$_{12}$O$_{40}^{3-}$ (collagen-PW$_{12}$O$_{40}^{3-}$)$_n$/cysteamine/Au electrode: The electrochemical behaviours of PW$_{12}$O$_{40}^{3-}$ (collagen-PW$_{12}$O$_{40}^{3-}$)$_n$/cysteamine/Au electrode was investigated in 0.1M H$_2$SO$_4$ solution. The corresponding cyclic voltammograms (CVs) were showed in Fig. 3A. The PW$_{12}$O$_{40}^{3-}$ (collagen-PW$_{12}$O$_{40}^{3-}$)$_4$/cysteamine/Au electrode showed three pairs of obvious redox peaks in 0.1M H$_2$SO$_4$ solution (curve a) as compared to collagen-PW$_{12}$O$_{40}^{3-}$/cysteamine/Au electrode (curve b), PW$_{12}$O$_{40}^{3-}$/cysteamine/Au electrode (curve c) and cysteamine /Au electrode (curve d), suggesting the three pairs of redox peaks resulted mainly from the immobilized PW$_{12}$O$_{40}^{3-}$. The three pairs of redox peaks corresponded to one-electron, two-electron and one-electron processes, respectively[26]. The peak-to-peak separations of three pairs of redox peaks were 8 mV (I-I'), 95 mV (II-II') and 6 mV (III-III'), respectively (Fig. 3B), showing a good reversibility. The peak currents increased linearly as the scan rates increased from 10-400 mV s^{-1} and the peak-to-peak separations were almost invariable as shown in Fig. 4, indicating the electron transfer reactions associated with a surface-confined process and the electron transfer was very fast. In addition, the peak current (taking the second anodic peak current as a representative) increased gradually as the numbers of layer increased (Fig. 5). In initial five layers, the increase of peak current was very slow. When the number of layers exceeded five layers, the increase of peak current became very fast. After seven layers, the peak current was invariable. This behaviour could be ascribed to the preparation of the modified electrode. As mentioned above, the collagen assembled on PW$_{12}$O$_{40}^{3-}$/cysteamine/gold electrode and formed collagen network. The PW$_{12}$O$_{40}^{3-}$ preferentially deposited on the collagen network and produced the PW$_{12}$O$_{40}^{3-}$ network. In the initial step of the electrode preparation, PW$_{12}$O$_{40}^{3-}$ networks resulted in a few collagen molecules assembled on the electrode surface. As the layers increased, the mesh of the network gradually decreased and consequently a large number of PW$_{12}$O$_{40}^{3-}$ assembled on the electrode surface. Therefore, the increase of peak current was slow firstly and then became very fast. After seven layers, the loading of collagen-PW$_{12}$O$_{40}^{3-}$ reached the maximum value and the peak current became constant.

According to Faraday's law, $I_p = nFQv/4RT = n^2F^2\Gamma^*v/4RT$, the surface average concentration of electroactive PW$_{12}$O$_{40}^{3-}$ (Γ^*, mol cm^{-2}) on the Au electrode was estimated as follows: $\Gamma^* = Q/nFA$, where I_p is the reduction current (A), v is scan
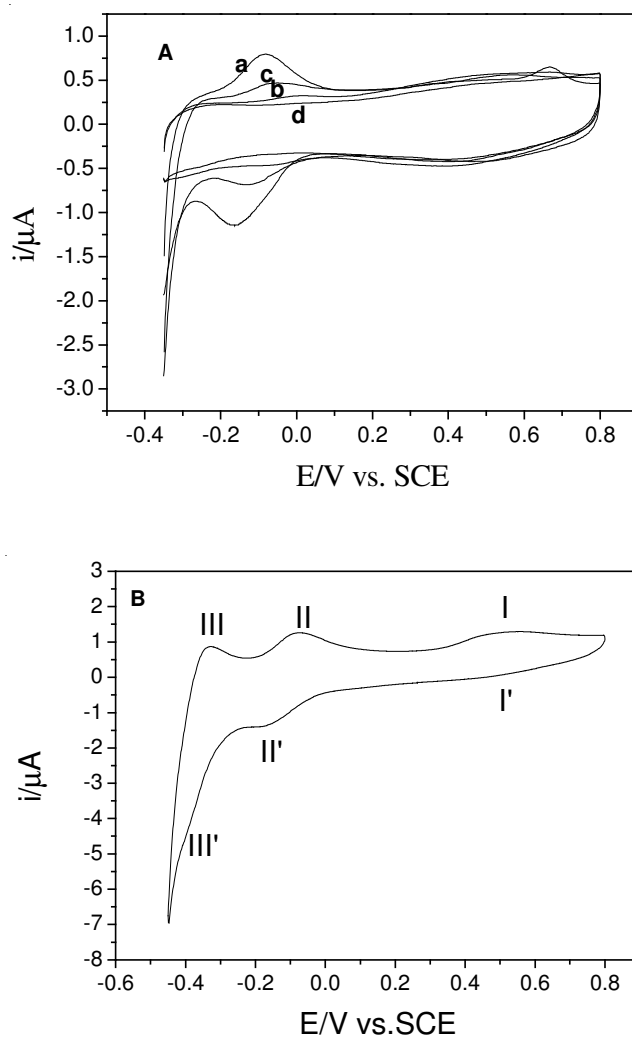

Fig 3.   (A) Cyclic voltammograms of various modified electrodes: PW$_{12}$O$_{40}^{3-}$ (collagen-PW$_{12}$O$_{40}^{3-}$)$_4$/cysteamine/Au electrode (a), collagen-PW$_{12}$O$_{40}^{3-}$/cysteamine/Au (b), PW$_{12}$O$_{40}^{3-}$/cysteamine/Au (c) and cysteamine/Au (d). (B) CVs of PW$_{12}$O$_{40}^{3-}$ (collagen-PW$_{12}$O$_{40}^{3-}$)$_4$/cysteamine/Au electrode in 0.1M H$_2$SO$_4$ solution. The scan rate was 50 mV s^{-1}
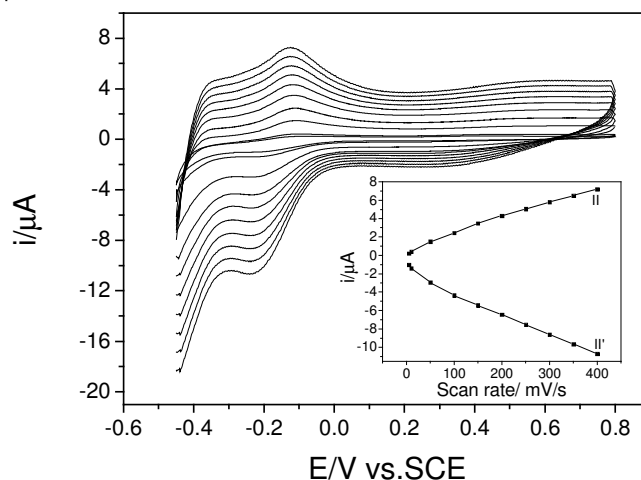
Fig. 4.   Cyclic voltammograms of the PW$_{12}$O$_{40}^{3-}$ (collagen-PW$_{12}$O$_{40}^{3-}$)$_4$/cysteamine/Au electrode in 0.1M H$_2$SO$_4$ solution at different scan rates (from inner to outer: 10, 50, 100, 150, 200, 250, 300, 350, 400 mV s^{-1}). The inset showed variation of the peak current with the scan rates
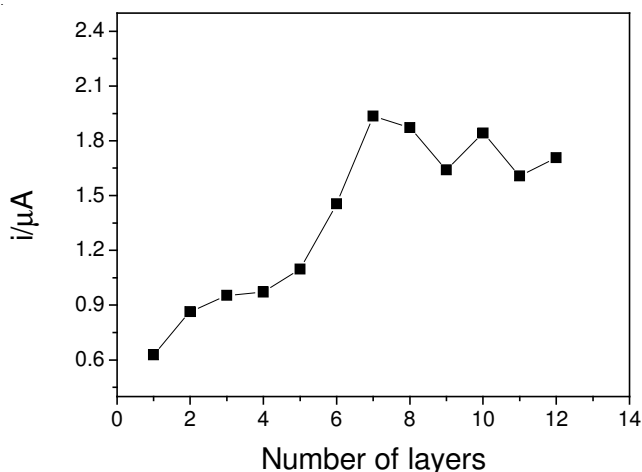
Fig. 5. Plots of anodic peak current (peak II) *versus* number of layers. The data were obtained in 0.1M H_2SO_4 solution at 50 mV s^{-1}
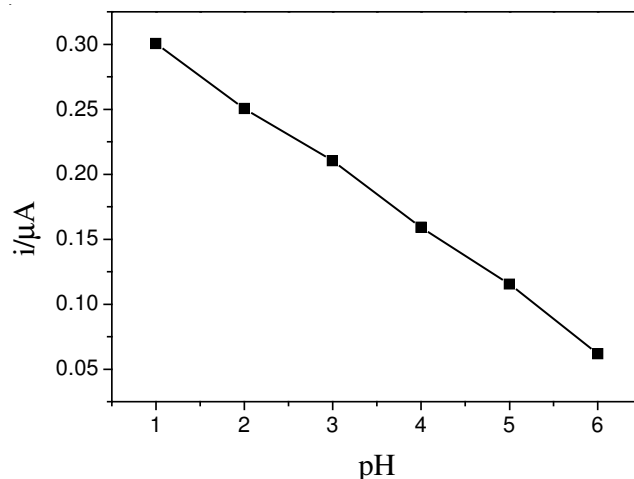

Fig. 6. Plots of anodic peak current (peak II) versus the pH. The data were obtained in 0.1M H_2SO_4 solution at 50 mV s^{-1}

rate (V s^{-1}), Q is the charge (C) by integrating of the anodic peak of the $PW_{12}O_{40}^{3-}$ modified electrode, n is the electron transfer number, F is the Faraday constant (F = 96493 C mol^{-1}) and A is the geometric area (cm^2) of the Au electrode (φ = 2 mm). The surface average concentration of electroactive $PW_{12}O_{40}^{3-}$ on the Au electrode were 4.2×10^{-12} mol cm^{-2} for $PW_{12}O_{40}^{3-}$/cysteamine/Au electrode and 3.48×10^{-11} mol cm^{-2} for $PW_{12}O_{40}^{3-}$(collagen-$PW_{12}O_{40}^{3-}$)$_4$/cysteamine/Au electrode, respectively (Table-1). The value of Γ^* increased with the number of layers increasing. Besides, the electron transfer rate k_s is also estimated according to $k_s = \alpha nFv/RT$, where α is the cathodic electron transfer coefficient, n is the electron transfer number, R is the gas constant (R = 8.314 J mol K^{-1}), T is the temperature in Kelvin (T = 298 K) and F is the Faraday constant[32]. The heterogeneous electron transfer rate of $PW_{12}O_{40}^{3-}$(collagen-$PW_{12}O_{40}^{3-}$)$_4$/cysteamine/Au electrode was similar to that of $PW_{12}O_{40}^{3-}$/cysteamine/Au electrode as shown in Table-1, suggesting the 3D porous structure was helpful to the electron transfer. Some other key parameters were also listed in Table-1.

Effect of pH on electrochemical behaviours of $PW_{12}O_{40}^{3-}$ (collagen-$PW_{12}O_{40}^{3-}$)$_4$/cysteamine/Au electrode: In general, the reduction of $PW_{12}O_{40}^{3-}$ was accompanied by protonation[33] and the assembly of the $PW_{12}O_{40}^{3-}$ (collagen-$PW_{12}O_{40}^{3-}$)$_4$/cysteamine/Au electrode was also based on the protonation of NH_2 of collagen and cysteamine. Thus, the pH of the solution might possibly play a crucial role in the electrochemical behaviours and stability of the $PW_{12}O_{40}^{3-}$ (collagen-$PW_{12}O_{40}^{3-}$)$_4$/cysteamine/Au electrode. As shown in Fig. 6, the peak currents decreased regularly with the increase of pH in the range of 1.0-6.0, suggesting the $PW_{12}O_{40}^{3-}$ (collagen-$PW_{12}O_{40}^{3-}$)$_4$/cysteamine /Au electrode only was stable in acidic solution.

Electrocatalytic activity of $PW_{12}O_{40}^{3-}$ (collagen-$PW_{12}O_{40}^{3-}$)$_4$/cysteamine/Au electrode: The $PW_{12}O_{40}^{3-}$ (collagen-$PW_{12}O_{40}^{3-}$)$_4$/cysteamine/Au electrode showed a good electrocatalytic activity toward the reduction of nitrite (NO_2^-). As shown in Fig. 7A, an obvious reduction current appeared when the $PW_{12}O_{40}^{3-}$ (collagen-$PW_{12}O_{40}^{3-}$)$_4$/cysteamine/Au electrode was scanned in 0.1M H_2SO_4 solution in the presence of 2 mM NO_2^- (curve e). This current is obvious as compared to that of in the absence of NO_2^- (curve a). The reduction current for cysteamine/Au electrode (curve b), $PW_{12}O_{40}^{3-}$/cysteamine/Au electrode (curve c) and collagen/$PW_{12}O_{40}^{3-}$/cysteamine/Au electrode (curve d) were obviously weak. The results suggested that the current resulted mainly from the $PW_{12}O_{40}^{3-}$ electrocatalytic reduction of NO_2^-. With the increase of NO_2^- in the electrolyte solution, the cathodic peak current (II', III') increased obviously while the corresponding anodic peak current (II, III) decreased and other peak was almost unchanged (Fig. 7B). At sufficiently acidic conditions, NO_2^- undergoes a disproportionation reaction leading to the formation of NO^+ (pKa = 3.3), which involves reductive centers in the polyoxometalate[34]. Therefore, the above result indicates that the second and the third redox processes catalyzed the reduction of NO_2^-, which corresponds to the reduction of $PW_{12}O_{40}^{4-}$ to $PW_{12}O_{40}^{6-}$ and $PW_{12}O_{40}^{6-}$ to $PW_{12}O_{40}^{7-}$, respectively.

The amperometric response of the $PW_{12}O_{40}^{3-}$(collagen-$PW_{12}O_{40}^{3-}$)$_4$/cysteamine/Au electrode toward the reduction of NO_2^- was studied by successive injections of NO_2^- with different concentration into a stirred 0.1M H_2SO_4 solution. Fig. 8 showed the typical current-time curve. The reduction current increased rapidly to achieve 95 % of the steady state current within 2 s after an aliquot of NO_2^- was added into the stirred solution. The fast response was attributed to the network structure of the modified electrode that could result in

TABLE-1
COMPARISON OF THE KEY PARAMETERS OF THE $PW_{12}O_{40}^{3-}$/CYSTEAMINE/Au AND
$PW_{12}O_{40}^{3-}$(COLLAGEN-$PW_{12}O_{40}^{3-}$)$_4$/CYSTEAMINE/Au ELECTRODES

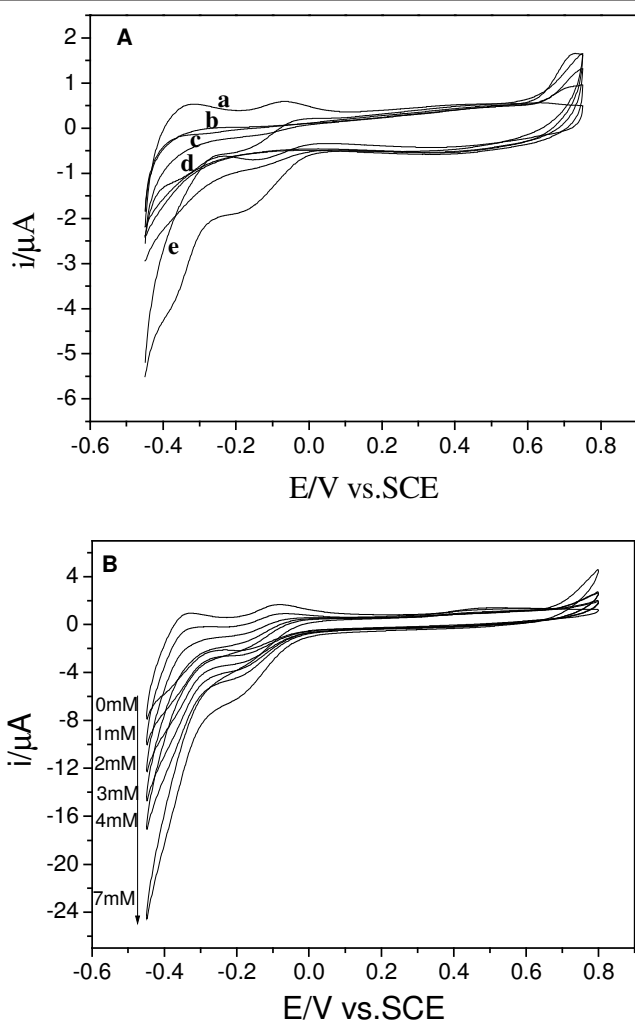|	Q (C)	Γ^* (mol cm^{-2})	k_s (s^{-1})	Linearity (mM)	Detection limit (μM)
$PW_{12}O_{40}^{3-}$/cysteamine/Au	2.55×10^{-8}	4.2×10^{-12}	2.82	0.14-33.94	1.71
$PW_{12}O_{40}^{3-}$(collagen-$PW_{12}O_{40}^{3-}$)$_4$/cysteamine/Au	2.11×10^{-7}	3.48×10^{-11}	2.80	0.14-51.94	1.29

Fig. 7.   (A) CVs of the $PW_{12}O_{40}^{3-}$ (collagen-$PW_{12}O_{40}^{3-}$)$_4$/cysteamine/Au electrode (a, e), cysteamine/Au electrode (b), $PW_{12}O_{40}^{3-}$/cysteamine/Au electrode (c), collagen-$PW_{12}O_{40}^{3-}$/cysteamine/Au electrode (d) in 0.1M H_2SO_4 solution containing 0 mM (a) and 2 mM NO_2^- (b, c, d, e). (B) CVs of the $PW_{12}O_{40}^{3-}$ (collagen-$PW_{12}O_{40}^{3-}$)$_4$/cysteamine/ Au electrode in 0.1M H_2SO_4 solution containing NO_2^- with various concentrations. Scan rate: 50 mV s^{-1}
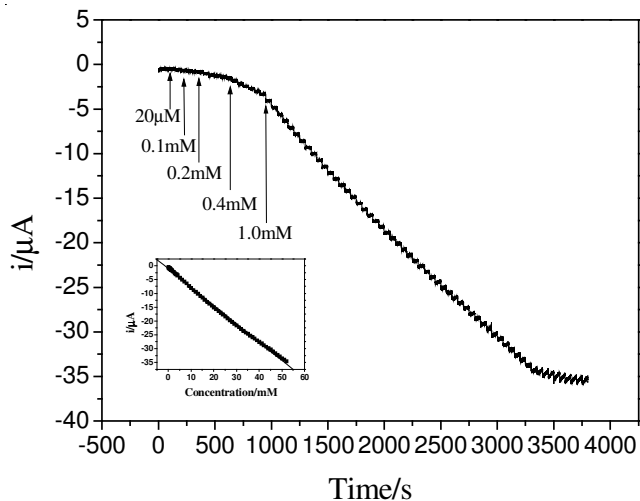

Fig. 8.   Amperometric response of the $PW_{12}O_{40}^{3-}$ (collagen-$PW_{12}O_{40}^{3-}$)$_4$/ cysteamine/Au electrode at -390 mV upon successive additions of different concentration NO_2^- into 0.1 M H_2SO_4 solution. Inset was plot of steady-state current *versus* NO_2^- concentration

fast penetration of the NO_2^-. The inset showed the calibration curve for reduction of NO_2^-. As the concentration of NO_2^- increased, the reduction current increased linearly. The response time is faster and the linear range (S/N = 3) is wider than the reported results of some other electrodes as sensors for NO_2^- detection as shown in Table-2. The comparison of the parameters of POMs and some other inorganic materials modified electrodes as sensors for NO_2^- were listed in Table-2.

Response of the sensor for the possible interfering materials: Possible interference is inevitable in the determination of NO_2^-. Some interfering agents were investigated by addition of them with different concentration into 1.0M H_2SO_4 solutions in the presence of 1 mM NO_2^-. As shown in Table-3, the common interfering agents such as KCl in a 1-fold concentration and Na_2SO_4 did not show interference to NO_2^- detection, while $KBrO_3$, KIO_3 and KCl in a 5-fold concentration displayed serious interference.

Stability of the $PW_{12}O_{40}^{3-}$(collagen-$PW_{12}O_{40}^{3-}$)$_4$/cysteamine/Au electrode: The stability of the $PW_{12}O_{40}^{3-}$ (collagen-$PW_{12}O_{40}^{3-}$)$_4$/cysteamine/Au electrode was investigated by the cyclic scan in 0.1M H_2SO_4 in the potential from -0.45 to 0.8 V at 50 mV s^{-1} (Fig. 9). The peak current only dropped by 8 % after fifty cycles and then maintained stable, which suggested the good stability of the modified electrode in such condition. Moreover, after the modified electrode was exposed to air at 4 ºC for 6 days, the peak current (I-I') increased 83 % while other peak currents (II-II', III-III') decreased 39 and 50 %, respectively (curve c).
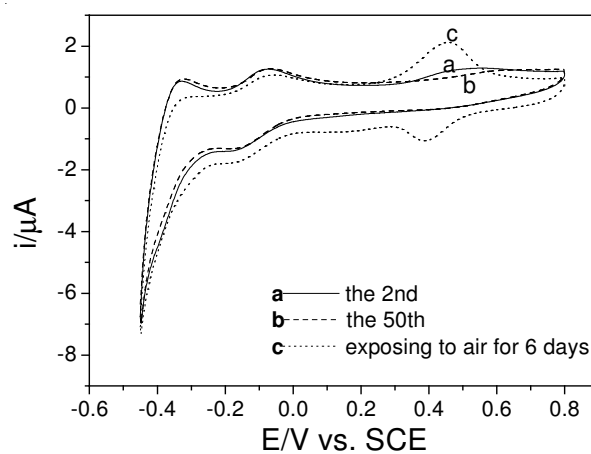

Fig. 9.   CVs of the $PW_{12}O_{40}^{3-}$ (collagen-$PW_{12}O_{40}^{3-}$)$_4$/cysteamine/Au electrode in 0.1M H_2SO_4 solution at 50 mV s^{-1} for 2 cycles (a) and for 50 cycles (b). (c) CVs of the $PW_{12}O_{40}^{3-}$ (collagen-$PW_{12}O_{40}^{3-}$)$_4$/ cysteamine/Au electrode exposed to air for 6 days in 0.1M H_2SO_4 solution at 50 mV s^{-1} for 2 cycles

Conclusion

A multilayer composed of type I collagen and $PW_{12}O_{40}^{3-}$ has been successfully fabricated on the cysteamine modified gold electrode surface by recycling the assembly of the type I collagen network and electrodeposition of the $PW_{12}O_{40}^{3-}$. The resulted $PW_{12}O_{40}^{3-}$ (collagen-$PW_{12}O_{40}^{3-}$)$_n$/cysteamine/Au electrode exhibited good electrochemical behaviours and electrocatalytic properties towards the reduction of NO_2^-. This sensor showed an extremely fast amperometric response, a low detection limit and a wide linear range for NO_2^- detection.

TABLE-2
COMPARISON OF THE PARAMETERS OF POMs AND SOME OTHER INORGANIC
MATERIALS MODIFIED ELECTRODES AS SENSORS FOR NO_2^-

	Response time (s)	Detection limit (μM)	Linear range (mM)	Sensitivity (μA mM^{-1})	Reference
$PW_{12}O_{40}^{3-}$ (collagen-$PW_{12}O_{40}^{3-}$)$_4$/cysteamine/Au	2	1.29	0.14-51.94	0.71	This paper
P_2W_{18}-modified sol-gel electrode	<10	5	0.02-34	3.25	27
P_2Mo_{18}/OMC/GC	<25	1.78	5.34×10^{-3}–24		28
POM-modified T-CPE		22	0.1-15		29
POM-modified IL-CPE		0.45	0.1-15		
PMo_{12}-l-Cys/Au		5	2×10^{-3}–0.2		17
PMo_{12}-AT/Au		0.02	10^{-4}-0.1		30
Tungsten oxide		700	1.6-20		31

TABLE-3
EFFECTS OF INTERFERENCES ON THE CATALYTIC REDUCTION OF NO_2^- TO FOLLOWING
SPECIES (RECORD IN 0.1M H_2SO_4, SCAN RATE 50 mV/s)

Responding substrates concentration: 1 mM	Interferences substrates (mM)						
	KCl		KBrO$_3$	KIO$_3$	Na$_2$SO$_4$		
	1	5	1	1	1	5	10
NO_2^-	o^a	●^{b}	●	●	o	o	o

a: No interference (variance of catalytic current ≤ 6 %); b: Interference (variance of catalytic current > 6 %).

REFERENCES

1. Z.M. Zhang, Y.F. Qi, C. Qin, Y.G. Li, E.B. Wang, X.T. Wang, Z.M. Su and L. Xu, *Inorg. Chem.*, **46**, 8162 (2007).
2. J.Q. Sha, J. Peng, A.X. Tian, H.S. Liu, J. Chen, P.P. Zhang and Z.M. Su, *Cryst. Growth Des.*, **7**, 2535 (2007).
3. M.C. Kuo, B.R. Limoges, R.J. Stanis, J.A. Turner and A.M. Herring, *J. Power. Sources*, **171**, 517 (2007).
4. I. Gatto, A. Sacca, A. Carbone, R. Pedicini, F. Urbani and E. Passalacqua, *J. Power. Sources*, **171**, 540 (2007).
5. E.B. Wang, C.W. Hu and L. Xu, Introduction to Polyacid Chemistry, Beijing: Chem Ind Press, Vol. 12, p. 125 (1998).
6. B. Keita, L. Nadjo and J. Saveant, *J. Electroanal. Chem.*, **243**, 105 (1988).
7. M.T. Pope and A. Miiller, *Angew. Chem. Int. Ed. Eng.*, l**30**, 34 (1991).
8. M. Sadakane and E. Steckhan, *Chem. Rev.*, **98**, 219 (1998).
9. M.A. Rahman, M.S. Won, P.H. Wei and Y.B. Shim, *Electroanalysis*, **18**, 993 (2006).
10. S.M. Chem and Y.H. Fa, *Electroanalysis*, **17**, 579 (2005).
11. A. Kuhn and F.C. Anson, *Langmuir*, **12**, 5481 (1996).
12. B. Keita, D. Bouaziz, L. Nadjo and A. Deronzier, *J. Electroanal. Chem.*, **279**, 187 (1990).
13. B. Keita, D. Bouaziz and L. Nadjo, *J. Electroanal. Chem.*, **255**, 307 (1988).
14. L. Cheng, L. Niu, J. Gong and S. Dong, *Chem. Mater.*, **11**, 1465 (1999).
15. J. Liu, L. Cheng, B. Liu and S. Dong, *Langmuir*, **16**, 7471 (2000).
16. L. Wang, M. Jiang, E.B. Wang, L.Y. Duan, N. Hao, Y. Lan, L. Xu and Z. Li, *J. Solid State Chem.*, **176**, 13 (2003).
17. S.F. Wang and D. Du, *Sens. Actuators B*, **94**, 282 (2003).
18. C. Chen, Y. Song and L. Wang, *Electrochim. Acta*, **54**, 1607 (2009).
19. C. Chen, Y. Song and L. Wang, *Electroanalysis*, **20**, 2543 (2008).
20. T. Koide, M. Yuguchi, M. Kawakita and H.J. Konno, *J. Am. Chem. Soc.*, **124**, 9388 (2002).
21. S.Z. Zong, Y. Cao, Y.M. Zhou and H.G. Ju, *Langmuir*, **22**, 8915 (2006).
22. C.C. Silva, A.G. Pinheiro, D. Thomazini, J.C. Goes, S.D. Figueiro, J.A.C. de Paiva and A.S.B. Sombra, *Mater. Sci. Eng. B.*, **83**, 165 (2001).
23. Y. Sun, G. Wei, Y. Song, L. Wang, L. Sun, C. Guo, T. Yang, Z. Liu and Z. Li, *Nanotechnology*, **19**, 115604 (2008).
24. Y. Song, K. Cui, L. Wang and S. Chen, *Nanotechnology*, **20**, 105501 (2009).
25. S.K. Dey, Y.T. Long, S. Chowdhury, T.C. Sutherland, H.S. Mandal, H.B. Kraatz, *Langmuir*, **23**, 6475 (2007).
26. Y.P. Shan, G.C. Yang, Y.T. Jia, J. Gong, Z.M. Su and L.Y. Qu, *Electrochem. Commun.*, **9**, 2224 (2007).
27. B. Wang, L. Cheng and S. Dong, *J. Electroanal. Chem.*, **516**, 17 (2001).
28. M. Zhou, L. Guo, F. Lin and H. Liu, *Anal. Chim. Acta*, **587**, 124 (2007).
29. H. Liu, P. He, Z. Li, C. Sun, L. Shi, Y. Liu, G. Zhu and J. Li, *Electrochem. Commun.*, **7**, 1357 (2005).
30. S. Wang, Y. Sun, X. Wang and X. Zhang, *Microchim. Acta*, **149**, 185 (2005).
31. I.G. Casella and M. Contursi, *Electrochim. Acta*, **50**, 4146 (2005).
32. J. Xu, F. Shang, J.H.T. Luong, K.M. Razeeb and J.D. Glennon, *Biosens. Bioelectron.*, **25**, 1313 (2010).
33. L.D. Li, W.J. Li, C.Q. Sun and L.S. Li, *Electroanalysis*, **14**, 368 (2002).
34. B. Keita, A. Belhouari, L. Nadjo and R. Contant, *J. Electroanal. Chem.*, **381**, 243 (1995).